Electric Arc Locator in Photovoltaic Power Systems Using Advanced Signal Processing Techniques

Angela Digulescu, Ion Candel, Jawad Dahmani, Cornel Ioana, Gabriel Vasile

Electric Arc Locator in Photovoltaic Power Systems Using Advanced Signal Processing Techniques

Angela Digulescu[1], Ion Candel[2,3], Jawad Dahmani[2], Cornel Ioana[2], Vasile Gabriel[2]
[1] Military Technical Academy, 34 – 39 George Cosbuc Avenue, Bucharest, Romania
[2] Gipsa-lab, Grenoble Institute of Technology, 11 rue des Mathématiques, BP 46, Saint Martin d'Hères, 38402, France
adigulescu@mta.ro
{ion.candel, jawad.dahmani, cornel.ioana, gabriel.vasile}@gipsa-lab.grenoble-inp.fr

Abstract – In this paper, we present two techniques for the localization of electric arcs produced in photovoltaic power systems. High order statistic analysis (HOSA) and recurrence plot analysis (RPA) have already proven successful in detecting the partial discharges associated with the production of an electric arc in a high voltage power system. However, this solves only the first half of the problem, since a localization of the arc also needed. Using a four sensors array detector along with a combination of HOSA and RPA techniques, we estimate the direction of arrival (DOA) of the electric arc, as well as the distance to the detector. An experiment was put in place in order to validate the results.

Keywords – High Order Statistics; bispectrum; fourth order cumulant; Recurrence Plot Analysis; phase space; direction of arrival; recurrence matrix; distance matrix;

I. INTRODUCTION

Fault detection in power systems is a major stake in the energy production and distribution chain. The rising amount of energy that has to be produced and distributed, along with equipment aging puts a heavy toll on the power systems all over the world. The occurrence of major faults increases dramatically with time and therefore it is essential to design a surveillance system consisting in fault detection and localization.

In [1] we have shown that electric arc (or partial discharge) detection in high voltage systems can be achieved using techniques based on polyspectra and RPA. HOSA and RPA are very robust to noise and interference and outperform previous techniques in terms of accuracy and computing time. Therefore, we have developed a technique to localize the electric arc based on a combination of RPA and HOSA.

The HOSA technique allows for a rapid and robust estimation of the DOA for an electric arc due to its rejection of signals with a Gaussian distribution [1]. Using the RPA method, we obtain very good results in estimating the distance from the electric arc to the locator.

Section 2 presents the theoretical aspects of the techniques used. In section three, we present the experimental configuration for generating electric arcs and in section four we illustrate the results of the localization using HOS and RPA. Section 5 contains the conclusions of our work so far, as well as the future developments.

II. HOSA AND RPA LOCALIZATION

A. HOSA localization

We model the system in figure 1 as an M equidistant receiver of P planar narrowband wave fronts [2]. The array output can be expressed as:

$$X(t)=\sum_{p=1}^{P}\int dS_p(\omega)e^{j\omega t}e(\omega;\theta_p)d\omega+V(t),$$
$$e_k(\omega;\theta_p)=\exp(-j\omega\tau_{pk}),\ \tau_{pk}=k(d\sin\theta_p)/c \quad (1)$$

where X(t) is an (Mx1) vector of sensor outputs, $\{dS_p(\omega)\}$ is the p^{th} received source signal with zero mean with a non Gaussian distribution. V(t) is an (Mx1) vector sensor noise considered independent and Gaussian and $e(\omega;\theta)$ is an (Mx1) directional vector for a source at bearing θ. The time delay, τ_{pk}, depends on the signal velocity, c, and the inter – sensor spacing, d. Our goal is to find a performance criteria related to the bispectral power [2]. First we calculate the covariance function of X(t) in order to obtain the third order cumulant and bispectrum representations of X(t):

$$R_X=\sum_{p=1}^{P}\int S_p(\omega)A(\omega;\theta_p)d\omega+\sigma_v^2, \quad (2)$$
$$A(\omega;\theta_p)=\left\{a_{k,s}(\omega;\theta_p)=e^{-j\omega(\tau_{pk}-\tau_{ps})}\right\}$$
$$C_X(\tau_1,\tau_2)=e^{j\omega_0(\tau_1+\tau_2)}\sum_p C_p(\tau_1,\tau_2)E_{\otimes}(\theta_p)$$
$$B_X(\omega_1,\omega_2)=\sum_p B_p(\omega_1,\omega_2)E_{\otimes}(\theta_p),$$

where R_X is the covariance function for X(t), $\{S_p(\omega)\}$ is the p^{th} received source signal power spectrum, $A(\omega;\theta)$ is MxM of directional elements, $C_p(\tau_1, \tau_2)$ and $B_p(\omega_1, \omega_2)$ are the p^{th} source third order cumulant and bispectrum; $E_{\otimes}(\theta_p)$ is the directional vector in the bispectral domain. The cross-bispectral power matrix of the random process X(t) becomes:

$$\Gamma_X=\iint C_X(\tau_1,\tau_2)B_X^H(\tau_1,\tau_2)d\tau_1 d\tau_2, \quad (3)$$

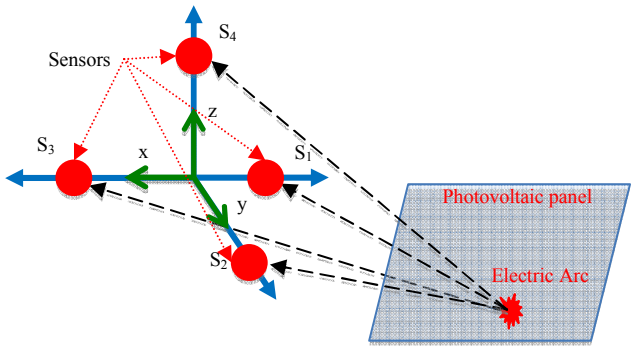

Figure 1. Schematics of electric arc on the photovoltaic panel and the arc locator.

The *cumulant beamformer* is defined as [3]:

$$P_1(\phi) = \iint \left\| E_{\otimes}^{T}(\phi) C_x(\tau_1, \tau_2) \right\|^2 d\tau_1 d\tau_2, \qquad (4)$$

where $-\pi/2 \le \varphi \le \pi/2$ is the angle bearing of the DOA and $E^T_{\otimes}(\varphi)$ is the steering vector in the bispectral domain.

If the array output contains unwanted non-Gaussian signals (reflections, electromagnetic interference, etc), we only allow the array output bispectral along the look direction to pass through while minimizing the bispectrum in other directions [2]. If we weight the bispectrum in the array output as $B_X(\omega_1, \omega_2) = w^T B_X(\omega_1, \omega_2)$, hence the constraint $w^T E^T_{\otimes}(\varphi) = 1$, this leads to the minimization of the following cost function, named the *optimum canceller spatial spectrum* [3]:

$$\begin{aligned} P_2(\phi) &= \iint \left\| B_X(\omega_1, \omega_2) \right\|^2 d\omega_1 d\omega_2 + \lambda\left(1 - z^T E_{\otimes}(\phi)\right) \\ &= \left[E_{\otimes}^{H}(\phi) \Gamma_X^{-1} E_{\otimes}(\phi) \right]^{-1} \end{aligned} \qquad (5)$$

where λ is a scalar Lagrange multiplier.

In [4] it is shown that using the model in (1), X(t) becomes an autoregressive (AR) model:

$$x(n) = -\sum_{k=1}^{P} a(k) x(n-k) + u(n), \qquad (6)$$

where u(n) is a non – Gaussian process. The linear bispectral estimate is also the maximum 3rd order entropy bispectral estimator [4]. The *maximum entropy cumulant spatial spectrum* becomes:

$$P_3(\phi) = \left\| E_{\otimes}^{H}(\phi) \Gamma_X^{-1} a \right\|^{-2}, \; a = [1\ 0\ \ldots\ 0_{M-1}], \qquad (7)$$

where a is the unit vector.

In section four, we give a comparison between the three HOSA based algorithms on estimating the DOA from real data.

B. *RPA localization*

As presented in [1], we first consider each received signal as a time series that is represented in the phase space. The trajectory described in the phase space is given by the vectors in (8):

$$v_l = \sum_{k=1}^{m} x\left(i + (k-1)d\right) e_k, \qquad (8)$$

where e_k are the versors of the phase space axes, x(.) are the data samples taken from the time series, d is the time delay parameter and m is the phase space dimension parameter.

The next step of the RPA method is to plot the distance/ recurrence matrix. Its computation (9) is based on the distance between points and on the trajectory. Generally, this trajectory is compared with a threshold (10) :

$$D(v_l, v_j) = \left\| v_l - v_j \right\|, \qquad (9)$$

$$R(i,j) = \Theta\left(\varepsilon(i) - D(v_l, v_j)\right), \qquad (10)$$

where $D(v_l, v_j)$ is the distance between points i and j, Θ represents the Heaviside step function and $\varepsilon(.)$ is the threshold of the recurrence plot. In other words, if we apply the Heaviside step function with a chosen $\varepsilon(.)$ on the distance matrix, we obtain a recurrence plot which points out if the distance between points i and j is lesser than $\varepsilon(.)$ or not. This is highlighted by black dots placed on the recurrence matrix. In most cases, ε is a constant and D represents the Euclidean metric.

We will not detail the choice of the delay parameter d, respectively the embedding dimension parameter m. This choice is rather critical, because they „draw" the distance/ recurrence matrix. As well as in [1], for the choice of the delay d, we have used the mutual information function, as for the choice of the embedding dimension m, we have used the farest nearest neighbor function. A more detailed approach can be found in [1], [5], [6].

In order to locate the electric arc, we first detect it, as in [1], on the distance matrix through the presence of a white horizontal/vertical band along the entire representation. It means that these few points are far enough from all other points from the received signal. The other points „draw" topologies which correspond to well known processes. In our application, we have uniformily diseminated signals which means that there is only noise.

Hereinafter, we have quantified the „image" of the process represented in the distance matrix through the summation of these effects, namely we have computed the sum of the elements of each column, as proposed in [1]:

$$sc(i) = \sum_{j=1}^{n-(m-1)d} D(v_l, v_j), \qquad (11)$$

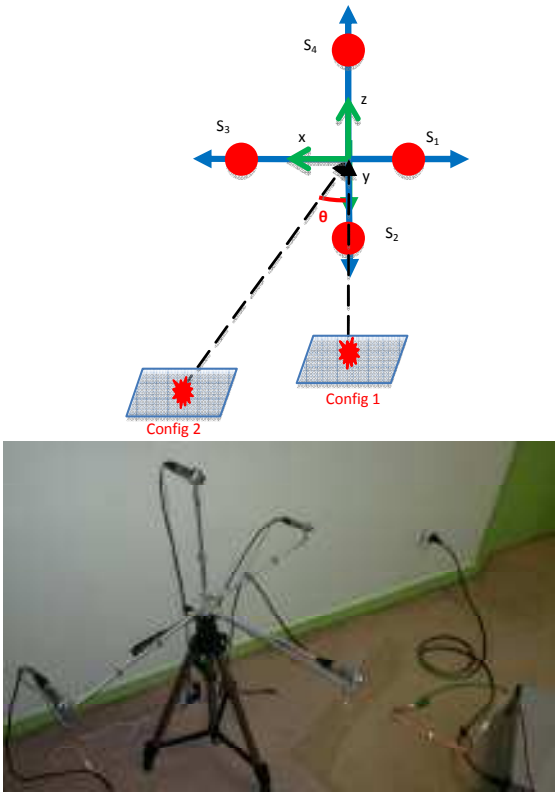

Figure 2. Electric arc locator experimental schematics (top) and practical implementation for Config1 (bottom) with electric arc.

where n is the length of the received signal used in the RPA computation. We will have therefore an ample peak for the sum of column corresponding to the white horizontal/ vertical band from the distance matrix, hence corresponding to the electric arc. So, we have detected the electric arc and also located it in time. The moment of arrival of the electric arc corresponds to the change of state from sc.

We have then normalised the sum (11) and chosen a threshold of 20% in order to correctly locate in time the arrival of the electric arc.

Accordingly, we have applied the RPA localization to each sensor and we have obtained four arrival times. Knowing the speed of sound in the air, it is only a matter of geometry to exactly locate the source, as in (12).

$$\begin{cases} d_{S_1p} - d_{S_2p} = vt_{12} \\ d_{S_2p} - d_{S_3p} = vt_{23} \\ d_{S_3p} - d_{S_4p} = vt_{34} \end{cases}, \qquad (12)$$

where $d_{S_ip} = \sqrt{\left(x_{S_i} - x_p\right)^2 + \left(y_{S_i} - y_p\right)^2 + \left(z_{S_i} - z_p\right)^2}$, i =1..4, S_i is the i^{th} sensor of the array. Also, P is the position of the source relative to the origin, v is the speed of sound in the air and $t_{ii+1} = t_i - t_{i+1}$, i = 1..3, where t_i is the arrival time corresponding to the sensor S_i.

III. Experimental Setup

We consider a four sensors 3D setup as illustrated in figure 2. Four acoustic sensors names S_1, S_2, S_3 and S_4 are placed in a 3D configuration (figure 2) so that it can receive the electric arc from a photovoltaic panel. Two electric arc configurations were simulated. First, the photovoltaic panel is placed in front of S_2 at a distance of 0.9 meters from the center of the detector along the y-axis. An electric arc was produced using a high voltage dielectric tester (figure 2). In the second configuration, the photovoltaic panel is situated 0.41 meters left from S_2 on the x-axis and 1 meter from the center of the detector on the y-axis. In both cases, signals were recorded using a high speed acquisition card. The DOA angle θ direction is considered as the y-axis of S_2. All DOA estimations will be made with respect of this direction.

IV. Results

A. HOSA results

For the first configuration, the theoretical angle θ = 0° and for the first configuration the theoretical angle θ = - 22.39°.

Practical estimations of DOA for the two configurations using the three estimators in (4), (5) and (7) are illustrated in figures 3 and 4:

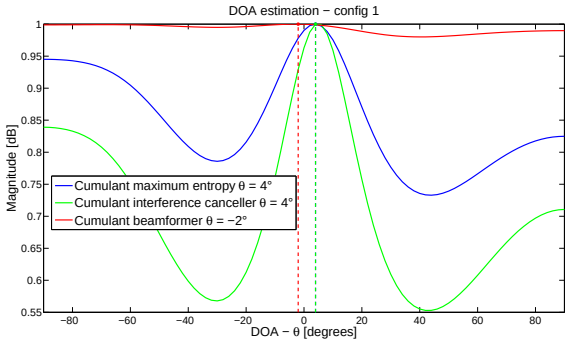

Figure 3. DOA estimation for the first configuration.

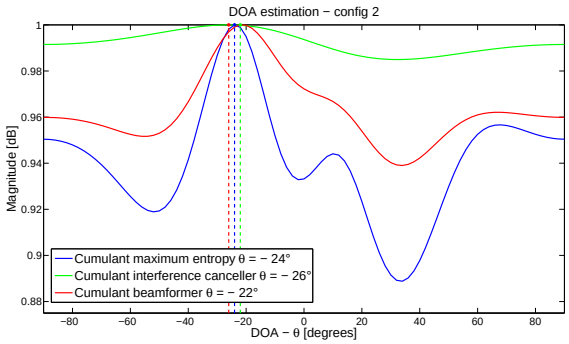

Figure 4. DOA estimation for the second configuration.

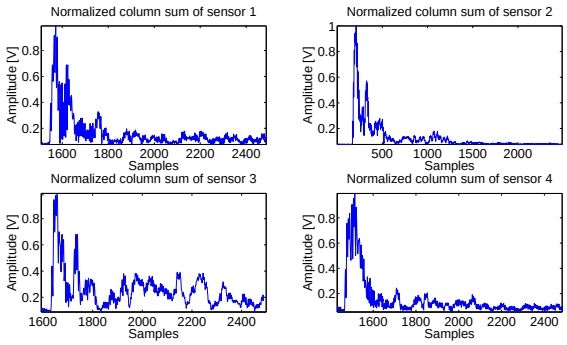

Figure 5. The normalized sum of each sensor – Config1.

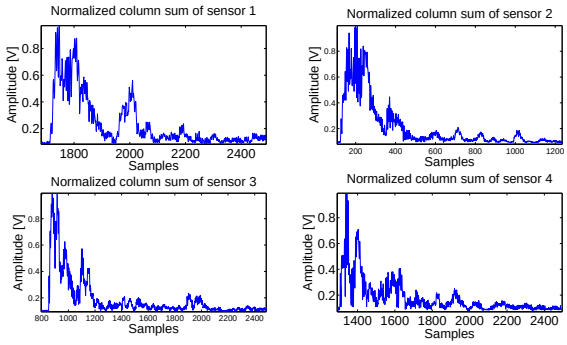

Figure 6. The normalized sum of each sensor – Config 2.

We see that the DOA angles obtained from the recorded data are slightly different from the theoretical values mentioned. This is due to the misalignment of the photovoltaic panels with the detector.

The results for both configurations have a maximum error $\Delta\theta = 4°$, which is acceptable in practical applications. However, as it can be seen in figure 4, the cumulant beamfomer described by (4) manages to provide an accurate estimation of the DOA for the second configuration and is closer to the theoretical DOA angle for the first configuration (see figure 3).

B. RPA results

We have applied the RPA method for the signals recorded from each sensor and computed the sum of columns on the distance matrix in order to detect and locate the electric arc. Only the samples corresponding to the electric arc's signature were considered, in order to reduce the computation time for the RPA method. Nevertheless, we have taken into account this fact in the arrival time. Thus, in the first configuration, we have the results presented in figure 5.

According to [1], for each normalized sum, we can discriminate the existence of the electric arc from all other signal. Moreover, we have shown in [1] that this can easily be done at a much lower SNR. Also, as shown in figure 5, it is easily to determine the moment of arrival of each electric arc, using, for example, a threshold. Having determined the arrival times, we have introduced them in the system expressed by (12). We have obtained the position of the source at P(x = 5cm, y = 82.42cm, z = 2.71cm). Thus, we have managed to locate the source with a precision of approximately ±5cm.

Concerning the second configuration, we have detected and located the electric arc considering the results highlighted by figure 6. In this case, we have obtained the position of the source at P(x = 33.95cm, y = 87.34cm, z = -3.55cm). The estimated coordinates have an error of ± 8cm.

V. CONCLUSIONS

With this paper, we have continued the previous work using HOSA and RPA for fault detection in power systems. HOSA provided three estimators of the bispectral power matrix that were used to detect the DOA of the electric arc from a photovoltaic panel.

For each estimator we have computed the DOA angle of an electric arc in two configurations. The results converged to the theoretical values in all three cases, the cumulant beamfomer being the most accurate of the three. Nevertheless, all three estimators can be successfully used in practical situations because the detector must indicate the area where the electric arc is produced.

The RPA localization manages successfully to detect and provide the distance to the detector. The main advantage of this method is its capability to process raw data (without the need for any pre-filtering) and to highlight very clear the electric arc and its moment of arrival in the normalized sum even if the SNR is low [1]. The differences appeared between the actual position of the source and the determined one have multiple causes: the accuracy of the measurements, the value of the considered speed of sound, acquisition timing, etc.

A combination between the two methods (HOSA and RPA) will translate into a very powerful, robust and accurate electric arc locator, with applications in all branches of energy systems. In the future, we will conduct an onsite measurement in order to test our detection and localization algorithms.

REFERENCES

[1] I. Candel, A.M. Digulescu, C. Ioana, A. Serbanescu, E. Sofron, G., "Optimization of partial discharge detection in high voltage cables based on advanced signal processing techniques," The 11th Conference on Information Science, Signal Processing and their Applications, ISSPA 2012, Montreal, Canada, July 3 – 5 2012.

[2] A.R. Leyman, T.S. Durrani, "HOS based detection of arrival estimation", Electronic letters, 31 March 1997, vol. 3, No. 7, pp. 540-541.

[3] A. T. Parsons, " Skewness in radiated noise," Internal report, UK Defense Agency, 1991.

[4] C. Y. Chi, "Linear prediction, maximum flatness, maximum entropy and AR polyspectral model," IEEE Transactions, 1993, SP-41, (6), pp 2155-2164.

[5] N. Marwan, S. Schinkel, J. Kurts, "Recurrence plots 25 years later – Gaining confidence in dynamic transitions," Europhysics Letters, 101, 20007, 2013

[6] A. Serbanescu, O. Stanasila, F. M. Birleanu, Analiza Non linear analysis of time series, Military Technical Academy Publishing, Bucharest, 2011